Ellipsometric investigation of $ZnFe_2O_4$ thin films in relation to magnetic properties

V. Zviagin, Y. Kumar, I. Lorite, P. Esquinazi, M. Grundmann, and R. Schmidt-Grund

Citation: Appl. Phys. Lett. **108**, 131901 (2016); doi: 10.1063/1.4944898
View online: https://doi.org/10.1063/1.4944898
View Table of Contents: http://aip.scitation.org/toc/apl/108/13
Published by the American Institute of Physics

Ellipsometric investigation of $ZnFe_2O_4$ thin films in relation to magnetic properties

V. Zviagin,[a] Y. Kumar, I. Lorite, P. Esquinazi, M. Grundmann, and R. Schmidt-Grund
Universität Leipzig, Institut für Experimentelle Physik II, Linnéstr. 5, D-04103 Leipzig, Germany

(Received 11 January 2016; accepted 16 March 2016; published online 28 March 2016)

We report an influence of disorder on structural and magnetic properties of $ZnFe_2O_4$ thin films grown at temperatures ranging from 400 °C to 600 °C by pulsed laser deposition in O_2 atmosphere on $SrTiO_3$ (100) substrates evidenced by properties of electronic transitions observed in the dielectric function. Inversion of the normal spinel structure was found to be one of the main mechanisms responsible for the increase in the magnetic response for the lowest growth temperature. The enhanced feature in the dielectric function located at ~3.5 eV, related to the transition involving tetrahedrally coordinated Fe^{3+} cations, corresponds to the dominating magnetic coupling between the octahedral and tetrahedral lattice sites, responsible for the overall ferrimagnetic behaviour of the film grown at the lowest temperature. © *2016 AIP Publishing LLC*.
[http://dx.doi.org/10.1063/1.4944898]

Spinel oxides are being extensively investigated and continue to receive a great amount of interest due to their wide range of possible high-frequency and high-power applications, including microwave, magnetic and magneto-optical recording devices, sensors, and electronic information mass storage.[1–3] $ZnFe_2O_4$ (ZFO) with a normal spinel ion distribution formula $[Zn_A^{2+}][Fe_B^{3+}]_2O_4^{2-}$, where A and B subscripts denote tetrahedral and octahedral lattice sites, respectively, is antiferromagnetic with a Néel temperature of about 10 K.[2] Depending on the deposition parameters and method, tunable electronic and magnetic properties are possible and are closely related to crystallographic properties.[1,4–7] However, the mechanism responsible for the observed ferrimagnetic behaviour at room temperature is still not fully understood, and two different arguments can be found, namely, spinel inversion[8] and defect induced magnetism due to cation and oxygen vacancies.[9] Both theories support the A-O-B interaction dominating over the B-O-B interaction resulting in the observed ferrimagnetic behaviour. Spectroscopic ellipsometry has been shown to be a useful technique to probe the electronic structure of the materials based on the optical transitions.[10–12] In this paper, we present a relation between the magnetic properties of ZFO and its electronic structure studied by spectroscopic ellipsometry and provide an explanation for the observed behavior which could shed light on the controversy in literature.

ZFO thin films were deposited on $SrTiO_3$ (100) substrates by pulsed laser deposition (PLD). A KrF excimer laser source ($\lambda = 248$ nm and pulse duration ~20 ns) was used to ablate the ZFO target, energy density of the laser beam on the target was kept around 2 J cm^{-2} with a repetition rate of 15 Hz. Films were grown at different temperatures, ranging from 400 °C to 600 °C and under oxygen partial pressure of $p_{O_2} = 0.016$ mbar. The pressure used was chosen in order to minimize and obtain similar concentration of oxygen vacancies for all the samples as determined from previous oxygen partial pressure dependent study for this material.[2] The crystalline structure of the samples was analysed by X-ray diffraction (XRD) $2\Theta - \omega$ scans using a wide-angle Phillips X'Pert Bragg-Brentano diffractometer with Cu K_α radiation. Magnetic properties were measured in a MPMS-7 superconducting quantum interference device (SQUID) from Quantum Design. The dielectric function, $\tilde{\varepsilon} = \varepsilon_1 + i\varepsilon_2$, of the thin films was determined by means of spectroscopic ellipsometry in a wide spectral range from 0.5 eV to 8.5 eV at room temperature and angles of incidence of 60° and 70°.[13] A commercial rotating analyzer spectroscopic ellipsometer, *J. A. Woollam Co. Inc.* VUV-VASE, in polarizer-compensator-sample-analyser (PCSA) configuration was used for this purpose. The ellipsometry spectra were analyzed by means of transfer matrix technique for a layer stack model containing a semi-infinite layer for the substrate, a layer for the spinel material, and a surface roughness layer, composed of a Bruggeman effective medium approximation mixture of the dielectric function of the thin film with 50% void, each described by its thickness and optical constants. Approximation calculation procedure is similar to the one presented in Ref. 10.

XRD $2\Theta - \omega$ scans for the investigated thin films are shown in Fig. 1. Along with the substrate peak, in the measured range, the (400)- and (800)-reflections corresponding to the spinel structure were observed with no additional observable secondary phases, which reveals highly oriented growth of deposited films. However, a shift in the film peak towards higher angle (Fig. 1(b)) confirms a reduction of the lattice parameter with increase in growth temperature. For 600 °C, it is closest to the bulk value of 8.44 Å.[1,14–17] The lattice constants of thin films, calculated by the Scherrer equation and extrapolated from $\cos^2(\Theta)$, are listed in Table I. Also, with increasing substrate temperature, an increase in peak intensity is apparent, stating an improvement of the crystallinity. These modifications in the lattice parameter and the crystallinity are possibly due to the variations in the cation disorder and/or oxygen vacancies and, therefore, there is a lattice relaxation towards normal spinel structure for highest deposition temperatures, considering similar surface roughness as

[a]Electronic mail: vitaly.zviagin@uni-leipzig.de

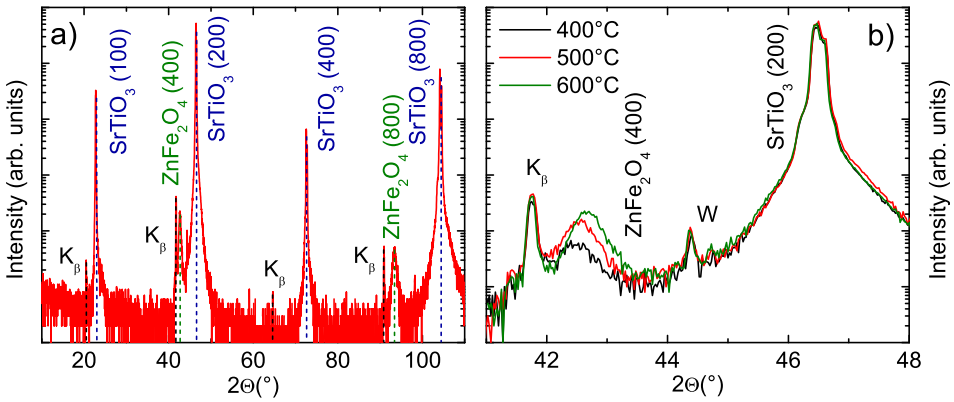

FIG. 1. XRD $2\Theta-\omega$ scans for ZFO thin film grown at 600 °C (a) and for the ZFO thin films for different growth temperatures (b). Substrate reflexes marked by K_β and W correspond to Cu K_β and W L_α spectral lines of the X-ray tube, respectively.

TABLE I. Calculated lattice parameter, thickness of the film and surface roughness, magnetization saturation M_{Sat} and magnetization remanence M_{Rem} measured at 5 K, transition energies for Gaussian (G) and critical point model (CPM0) along with the amplitude for G_2 as well as the amplitude ratio, $G_2/(G_1+G_3)$, listed for each growth temperature. The error estimated for the specified values is in the range of the last digit. The boldface numbers correspond to magnetization values and values obtained from the model dielectric function used in Figure 2(c).

Growth temperature (°C)	Lattice constant (Å)	Film thickness (nm)	Surface roughness (nm)	M_{Sat} (emu/g)	M_{Rem} (emu/g)	G_1 (eV)	CPM0 (eV)	G_2 (eV)	G_2 Amp ([1])	G_3 (eV)	Amp Ratio	G_4 (eV)	G_5 (eV)	G_6 (eV)
400	8.54	40.3	1.6	**60.89**	**35.98**	2.72	2.89	3.38	**1.25**	3.81	0.68	5.36	5.84	6.84
500	8.51	41.7	1.3	**27.80**	**15.73**	2.51	2.72	3.49	**0.44**	3.98	0.46	5.27	5.71	6.19
600	8.49	41.0	1.4	**21.66**	**11.49**	2.50	2.72	3.54	**0.29**	3.98	0.30	5.27	5.70	6.33

well as the thickness of the samples, Table I.[5] Changes are more evident for the increase in growth temperature from 400 °C to 500 °C, being smaller for further increase up to 600 °C. The film deposited at a substrate temperature of 300 °C was found to be X-ray amorphous.

Magnetization of thin films as a function of the applied magnetic field is shown for 5 K and 300 K in Fig. 2. Here, data are presented after subtracting the diamagnetic contribution from the substrate. It is visible from the B-H curves that all the samples exhibit ferrimagnetic order. Magnetization

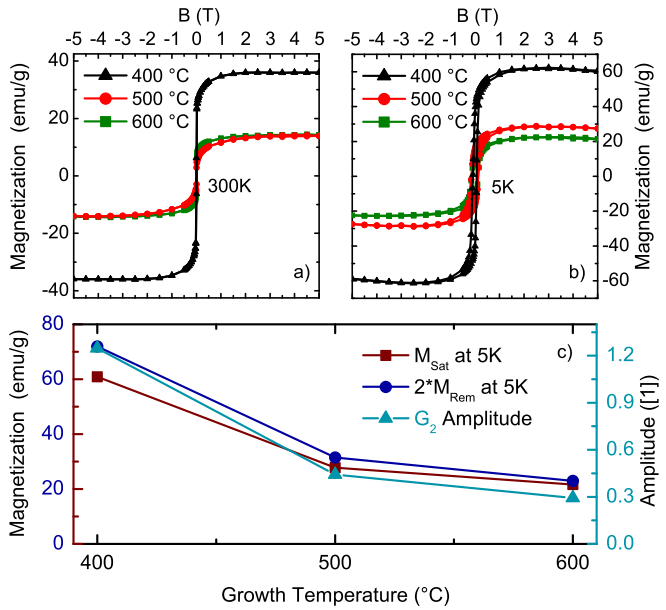

FIG. 2. Magnetization as a function of applied magnetic field at room temperature (a) and at 5 K (b) with deposition temperature indicated. Saturation and twice of remanence magnetization measured at 5 K as well as the amplitude of the transition involving tetragonally coordinated Fe^{3+} ions obtained from the model dielectric function versus growth temperature (c).

has been found to be reduced with increase in the deposition temperature (see Table I). It is in coincidence with the variation in the crystallinity and the lattice parameter observed in XRD, i.e., the variation is significant between the samples prepared at 400 °C and 500 °C, while a small decrease in magnetization with further increase in growth temperature (600 °C) is visible only for measurements at 5 K (Fig. 2(b)).

To understand this variation of magnetization with the deposition temperature, we determined the dielectric function of all samples using spectroscopic ellipsometry. For an optically isotropic sample, the measured ellipsometric quantities Ψ and Δ are defined by the ratio $\rho = r_p/r_s = \tan\Psi \exp(i\Delta)$ of the complex reflection coefficients of p- and s-polarized light, r_p and r_s, respectively. The ratio is related to the real and imaginary parts of complex reflectivity. The experimental data were modelled by means of parametric model dielectric function (MDF), developed for the entire spectral range for the films as well as for the substrate, consisting of a series of 7 contributing functions, namely, M0-critical point model functions (CPM0) and Gaussian oscillators.[18] Regression analysis was applied to best match the parametric MDF to the numerically inverted MDF. Based on the resonance energies, transitions were assigned from previous studies of the optical as well as magneto-optical properties of this material.[10–12] The absorption coefficient as well as the Kramers-Kronig consistent optical constants, calculated from the parametric MDF approximation, along with the individual contributions to the model are shown in Figs. 3 and 4, respectively. Transition energies for each oscillator and relevant amplitudes are listed in Table I, (see supplementary material for further details[19]).

Fig. 3 shows the deduced absorption coefficient for the three thin films. A clear difference of the absorption bands is visible for the three films with the main features located at ~3.9 eV and ~6.1 eV. Low absorption below ~2 eV

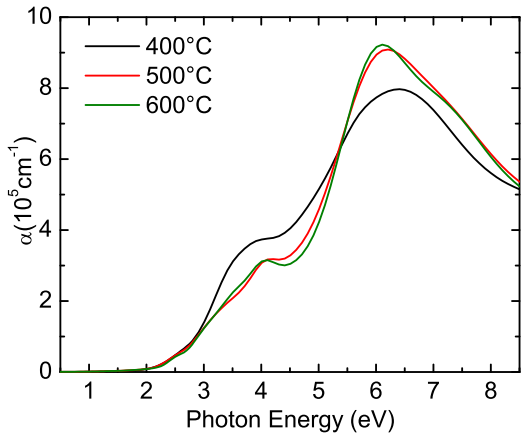

FIG. 3. Absorption coefficient α derived from numerical inversion for ZFO deposited at temperatures indicated.

demonstrates low concentration of Fe^{3+}-Fe^{2+} exchange in our insulating ZFO thin films in contrast to materials such as Fe_3O_4 and conducting ZFO having a strong absorption in that spectral range.[5,10–12] Features visible in the MDF, Fig. 4 (top panel), mainly correspond to transitions between the O_{2p} band and bands of Fe^{3+} and Zn^{2+} cations. While features below ~4.5 eV, G_1, G_2, G_3, correspond to transitions involving 3d bands of Fe^{3+} cations, above this energy, G_4, G_5, and G_6, correspond to transitions from O_{2p} band to 4s as well as higher lying bands of Fe^{3+} cation and from O_{2p} band to 4s band of Zn^{2+} cation, respectively.

As observed in Fig. 4 (inset), there is a redshift of the band placed at G_1 as well as a blueshift for the band at G_3 which is more evident from 400 °C to 500 °C. These bands arise from crystal field split states with Δ_{Oh} ($=10Dq$) of ~1.09 eV and ~1.48 eV for samples grown at 400 °C and 600 °C, respectively. With the latter value being closest to the bulk data and experimental values, corresponding to least amount of distortion,[20,21] Δ_{Oh} suggests a crystal field splitting between the two different bands and is related to transitions from the O_{2p} band to t_{2g} and e_g bands of the octahedral Fe_{3d} cations.

The transition located at G_2 hints to the presence of Fe^{3+} on tetrahedral lattice sites and serves as evidence for

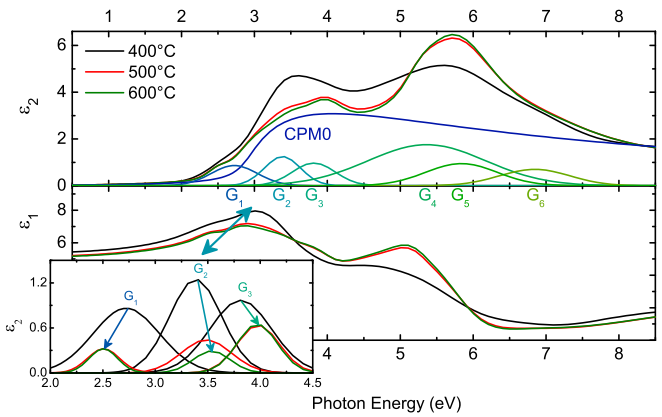

FIG. 4. Real part (bottom) and imaginary part (top) of the Kramers-Kronig consistent optical constants calculated from the parametric model for ZFO thin films grown at indicated temperatures. Color coded individual contributions to the parametric model for ε_2 are shown for the sample deposited at the lowest temperature. The inset shows change in amplitude of three oscillators, G_1, G_2, and G_3, with respect to the deposition temperature.

disorder within the crystal structure. Prior studies have shown the highest magneto-optical response of this peak for ZFO thin films grown at low temperature and thus relate this feature to a transition either from O_{2p} to tetrahedrally coordinated Fe^{3+} cation or to an inter-sublattice (A-B) charge transfer transition.[10,12,22,23] This peak becomes more pronounced as the normal spinel becomes more inverted and is the highest for Fe_3O_4 and $Li_{0.5}Fe_{2.5}O_4$ inverse spinel materials.[22–25] The increase in oscillator amplitude of this transition with decreasing growth temperature is directly related to the increase in saturation magnetization as well as the remanence magnetization measured at 5 K (Fig. 2(c) and Table I).

Since the increase of the oscillator amplitude of G_2 is greater than the amplitude increase of G_1 and G_3 with decreasing deposition temperature, see inset of Fig. 4 and amplitude ratio in Table I, two phenomena are possible. Firstly, a possible inversion mechanism where Zn^{2+} moves to the octahedral site and Fe^{3+} moves to the tetrahedral site, with decreasing growth temperature, thus following Eq. (1), where x is the inversion coefficient corresponding to the degree of cation disorder

$$[Zn^{2+}_{1-x}Fe^{3+}_{x}]_A[Zn^{2+}_{x}Fe^{3+}_{2-x}]_B O^{2-}_4. \quad (1)$$

On the other hand, presence of Fe^{3+} cations on nominally unoccupied tetrahedral sites is also possible and has been investigated in previous works.[8,26,27] Nonetheless, the presence of Fe^{3+} cations on tetrahedral sites leads to the ferrimagnetic pair coupling to be dominant over the antiferromagnetic pair coupling, resulting in the increase of ferrimagnetic magneto-static behaviour.

In summary, we have shown a variation of the magneto-static properties of ferrite thin films as a function of the growth temperature. The changes have been related to the changes in the octahedral and tetrahedral site occupancy as suggested by spectroscopic ellipsometry. Namely, the presence of Fe^{3+} cations located on tetrahedrally coordinated lattice sites serves as a reasonable explanation for the observed increase in magnetization saturation and remanence with decreasing growth temperature.

We gratefully acknowledge Gabriele Ramm for PLD target preparation and thickness determination, Holger Hochmuth for the thin film growth, and Annette Setzer for XRD measurements. We would like to thank Claudia Rodriguez Torres for carefully reading of the manuscript and useful comments. This work was funded by the Collaborative Research Center SFB762 "Functionality of Oxide Interfaces."

[1]A. A. Timopheev, A. M. Azevedo, N. A. Sobolev, K. Brachwitz, M. Lorenz, M. Ziese, P. D. Esquinazi, and M. Grundmann, Thin Solid Films **527**, 273 (2013).
[2]Y. F. Chen, D. Spodding, and M. Ziese, J. Phys. D: Appl. Phys. **41**, 205004 (2008).
[3]R. Valenzuela, Phys. Res. Int. **2012**, 591839 (2012).
[4]F. K. Lotgering, J. Phys. Chem. Solids **27**, 139 (1966).
[5]K. Brachwitz, T. Böntgen, M. Lorenz, and M. Grundmann, Appl. Phys. Lett. **102**, 172104 (2013).
[6]D. Venkateshvaran, M. Althammer, A. Nielsen, S. Geprägs, M. S. Ramachandra Rao, S. T. B. Goennenwein, M. Opel, and R. Gross, Phys. Rev. B **79**, 134405 (2009).
[7]J. Wu, N. Li, J. Xu, Y. Jiang, Z. G. Ye, Z. Xie, and L. Zheng, Appl. Phys. Lett. **99**, 202505 (2011).

[8]S. Nakashima, K. Fujita, K. Tanaka, K. Hirao, T. Yamamoto, and I. Tanaka, Phys. Rev. B **75**, 174443 (2007).
[9]C. E. Rodriguez Torres, G. A. Pasquevich, P. Mendoza Zélis, F. Golmar, S. P. Heluani, S. K. Nayak, W. A. Adeabo, W. Hergert, M. Hoffmann, A. Ernst, P. Esquinazi, and S. J. Stewart, Phys. Rev. B **89**, 104411 (2014).
[10]V. Zviagin, P. Richter, T. Böntgen, M. Lorenz, M. Ziese, D. R. T. Zahn, G. Salvan, M. Grundmann, and R. Schmidt-Grund, Phys. Status Solidi B **253**, 429 (2016).
[11]T. Böntgen, K. Brachwitz, R. Schmidt-Grund, M. Lorenz, and M. Grundmann, J. Appl. Phys. **113**, 073503 (2013).
[12]E. Liskova-Jakubisova, S. Visnovsky, P. Siroky, D. Hrabovsky, J. Pistora, S. C. Sahoo, S. Prasad, N. Venkataramani, M. Bohra, and R. Krishnan, J. Appl. Phys. **117**, 17B726 (2015).
[13]H. Fujiwara, *Spectroscopic Ellipsometry: Principles and Applications* (John Wiley and Sons, 2007).
[14]H. Yao and C. H. Yan, J. Appl. Phys. **85**, 6717 (1999).
[15]C. D. Spencer and D. Schroeer, Phys. Rev. B **9**, 3658 (1974).
[16]J. D. Hanawalt, H. W. Rinn, and L. K. Frevel, Ind. Eng. Chem., Anal. Ed. **10**, 457 (1938).
[17]T. R. Paudel, A. Zakutayev, S. Lany, M. dAvezac, and A. Zunger, Adv. Funct. Mater. **21**, 4493 (2011).
[18]T. Tiwald and J. A. Woollam, Co., Inc., *Addendum Software Manual WVASE32* [textregistered], 2001.
[19]See supplementary material at http://dx.doi.org/10.1063/1.4944898 for further details concerning parameters of parametric MDF.
[20]C. Himcinschi, I. Vrejoiu, G. Salvan, M. Fronk, A. Talkenberger, D. R. T. Zahn, D. Rafaja, and J. Kortus, J. Appl. Phys. **113**, 084101 (2013).
[21]K. J. Kim, H. S. Lee, M. H. Lee, and S. H. Lee, J. Appl. Phys. **91**, 9974 (2002).
[22]G. S. Krinchik, K. M. Mukimov, Sh. M. Sharipov, A. P. Khrebtov, and E. M. Speranskaya, Sov. Phys. - JETP **49**, 1074 (1979).
[23]G. S. Krinchik, A. P. Khrebtov, A. A. Askochenskii, E. M. Speranskaya, and S. A. Belyaev, Sov. Phys. - JETP **45**, 366 (1977).
[24]S. Visnovsky, V. Prosser, R. Krishnan, V. Parizek, K. Nitsch, and L. Svobodova, IEEE Trans. Magn. **17**, 3205 (1981).
[25]S. Visnovsky, N. P. Thuy, J. Stepanek, V. Prosser, and R. Krishnan, J. Appl. Phys. **50**, 7466 (1979).
[26]C. E. Rodriguez Torres, F. Golmar, M. Ziese, P. Esquinazi, and S. P. Heluani, Phys. Rev. B **84**, 064404 (2011).
[27]J. H. Shim, S. Lee, J. H. Park, S. J. Han, Y. H. Jeong, and Y. W. Cho, Phys. Rev. B **73**, 064404 (2006).